Photooxidation of Organic Chemicals Catalyzed by Nanoscale MoS_2

T. R. Thurston and J. P. Wilcoxon*

Sandia National Laboratories, Albuquerque, New Mexico 87108

Received: May 21, 1998

We describe experiments that explore the use of nanosize MoS_2 semiconductors for catalyzing the photooxidation of an organic chemical, phenol. The band gap of nanoscale MoS_2 can be tuned across the visible spectrum and we show that $d = 4.5$ nm MoS_2 which has an absorbance edge near 550 nm photooxidizes phenol using only visible light (>450 nm) while smaller band gap $d = 8-10$ nm MoS_2 or wide band gap Degussa P-25 TiO_2 do not. The possibility of increasing the rate of photooxidation of phenol by deposition of nanoclusters of MoS_2 on bulk semiconductor powders is investigated. It is shown that small amounts (<5 wt %) of nanoscale MoS_2 deposited onto TiO_2 can lead to significant (∼2-fold) enhancements of phenol destruction rates compared to TiO_2 by itself.

1. Introduction

The electron−hole pairs generated by solar radiation in semiconducting materials can catalyze redox reactions that destroy organic chemicals, a process with obvious environmental remediation potential. A significant amount of research on semiconductor-catalyzed photooxidation of organic chemicals has consequently been done during the past 15 years; reviews of this previous work are given in the Reference section.[1−6] Most studies have examined the photocatalytic activity of TiO_2. This material has shown great promise, with many beneficial characteristics including (a) the ability to catalyze the destruction of a wide variety of organic chemicals, (b) complete oxidation of organics to CO_2 and dilute mineral acids in many cases, (c) lack of inherent toxicity, (*d*) resistance to photodegradation, and (e) cheapness. Despite all these propitious properties, TiO_2-based photooxidation technology has still not been commercialized.

Two major disadvantages of TiO_2-based photooxidation technology are the lack of adequate fixed bed reactor designs and the large band gap of TiO_2 (∼3.2 eV). The former problem seems solvable soon; however, the latter problem is much more difficult to circumvent. Figure 1 illustrates the band gap issue. This plot shows the spectral irradiance of the solar spectrum at the earth's surface as a function of photon wavelength, along with the band gap wavelength of some of the materials examined in this work. Only photons with wavelengths smaller than the band gap wavelength can excite electron−hole pairs. For bulk TiO_2, this wavelength is in the near-UV region, ∼390 nm, which means that only a tiny fraction (∼3%) of the solar spectrum can be harvested. This deficiency was quickly recognized, and previous efforts[1−6] to ameliorate this problem have involved coating the TiO_2 with photosensitizers such as dyes. It is not clear that this approach will ultimately be commercially viable, however, since the dye molecules themselves can be photooxidized.

In this work we explore the photocatalytic properties of a possible alternative to TiO_2, nanosize MoS_2. We chose to investigate this particular material for several reasons. In bulk MoS_2, which has an anisotropic, layered, graphite-like structure consisting of S−Mo−S sandwiches held together by weak van der Waals forces, the electronic states of the conduction and valence bands are both derived primarily from Mo 4d orbitals. Photoexcitation of electrons therefore should not significantly weaken bonds between the Mo and S atoms, which leads to enhanced photodegradation resistance. Indeed, previous researchers have shown that defect-free bulk MoS_2 is remarkably photostable during photoelectrochemical oxidation of water.[7,16] When photooxidation of bulk electrodes of MoS_2 does occur it happens at step defects in the semiconductor film where Mo edge-site atoms are not protected by the inert basal planes of sulfur atoms and this results in dissolution of the lattice via oxidation of sulfur to sulfate ions. However, this process is quite slow in this covalent material compared to ionic semiconductor electrodes such as CdS.

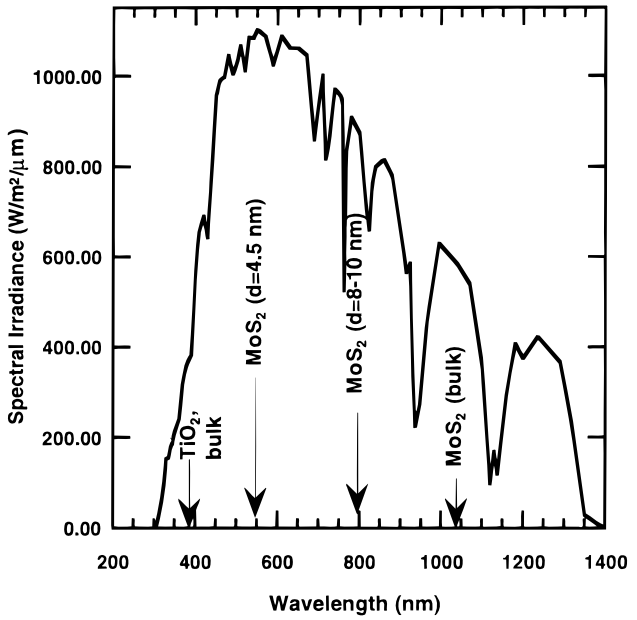

Figure 1. Spectral irradiance of the solar radiation that reaches the earth's surface as a function of photon wavelength (AM1.5D). The dips in the spectrum arise from absorbance in the earth's atmosphere. The absorbance edge of various semiconductor compounds examined in this work are also shown.

* Author to whom correspondence should be addressed.

10.1021/jp982337h CCC: $18.00
Published on Web 12/16/1998

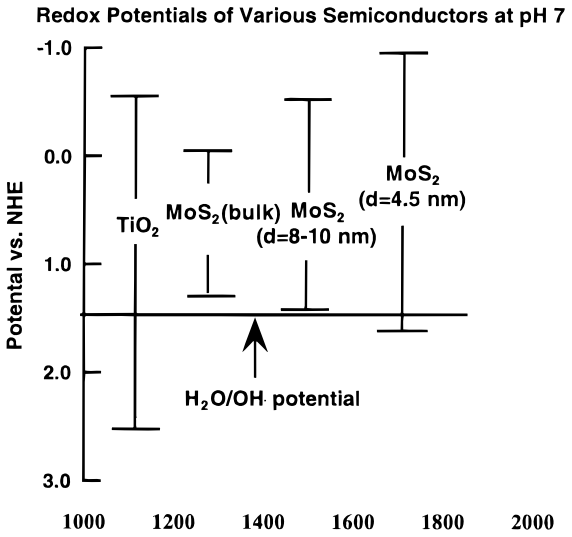

Figure 2. Position of the conduction and valence band edges vs normal hydrogen electrode (NHE) for bulk TiO_2 and MoS_2 of various sizes. If the valence band edge is more positive than +1.2−1.5 V, photogenerated holes can oxidize water and create hydroxyl radicals which can then oxidize dissolved organic chemicals.

The valence band of CdS, though thermodynamically stable compared to water oxidation, is kinetically unstable. The instability to photooxidation of the lattice is partially due to the ionic character of this semiconductor which means that the valence band is derived primarily from S 3p orbitals and the conduction band from Cd 5s orbitals. Not surprisingly, CdS readily photodegrades, releasing toxic cadmium ions upon illumination.[8] Nevertheless, Gratzel[9] has shown that for other photooxidation reactions, such as H_2S oxidation to elemental sulfur, the different kinetic pathway prevents photooxidation of the lattice. So, the issue of photostability in any semiconductor system is primarily kinetic, not thermodynamic as was recently pointed out by Tributsch in an excellent review article.[10]

An advantage of MoS_2 compared to photostable, wide-gap metal oxides such as TiO_2 is that the band gap of MoS_2 is small enough to allow most of the solar spectrum to be harvested. As discussed below, only nanoscale MoS_2 clusters are photochemically active for $\lambda > 400$ nm, and these materials can have their band gaps shifted from the bulk value by various amounts by quantum size effects. For example, the bulk indirect absorbance edge of MoS_2 is ∼1040 nm while a solution of 4.5 nm MoS_2 nanoclusters absorbs visible light starting at ∼550 nm.[11,12] Figure 1 illustrates this effect for some of the nanoclusters examined in this work. So a large fraction of the solar spectrum can be harvested by these nanoscale semiconductors.

Quantum size effects that increase the band gap in nanoscale MoS_2 also shift the redox potentials of the conduction and valence bands in advantageous ways. We have recently estimated the size of this effect by studying the kinetics of electron transfer to bipyridine.[14] A potential energy shift is necessary for MoS_2 to function as a photooxidation catalyst. This issue is illustrated in Figure 2, which shows the redox potentials of TiO_2 and MoS_2 (based upon the lowest energy indirect transition in both materials) of various sizes versus the normal hydrogen electrode potential (NHE). For TiO_2, the oxidation process appears to be dependent on the formation of surface-adsorbed hydroxyl radicals (•OH) from adsorbed water by valence band holes, with a corresponding reduction of dissolved molecular oxygen by conduction band electrons (provided no other reducible species is present). At pH = 7 solution, the production of •OH radicals will occur if the semiconductor valence band potential is larger than +1.20−1.5 V. A possible mechanism for •OH production is Mo(IV)...H_2O + h^+ = Mo(IV)-OH + H^+, which, for the analogous Ti(IV) system in TiO_2, has a redox potential of 1.5 ± 0.3 V vs NHE.[15] This will occur at the abundant Mo edge sites of a nanocluster. Another possible source of •OH production can occur by hole transfer from nanosize MoS_2 to bound H_2O in the presence of O_2 to produce hydrogen peroxide. This has a redox potential of ∼1.2 V vs NHE.[16]

It is easy to understand why only nanoscale MoS_2 will be catalytically active. As shown in Figure 2, the oxidation potential of bulk MoS_2 is not sufficiently large to produce •OH radicals. On the other hand, the same quantum size effects that increase the band gap in nanoscale MoS_2 will also shift the valence band enough to permit •OH production. In addition, the shift of the reduction potential to more negative values should accelerate the transfer of electrons to dissolved oxygen to form chemical species that will also attack organic molecules.

A significant advantage of nanocluster semiconductor particles is that the surface trapping of electrons and holes before recombination may be more efficient in small particles. The photogenerated electron−hole pairs have a much shorter distance to travel to reach the surface in a small cluster. Once the electrons and holes have been trapped at the interface, they can then participate in redox reactions.

Nanoparticles of the size of the MoS_2 in this work also scatter negligible amounts of light. Unlike slurries of bulk semiconductor powders which intensely multiply scatter all the incident light, light extinction in solutions of semiconductor nanoclusters occurs solely via absorbance. This may make understanding and modeling their photocatalytic behavior simpler.

The organization of this paper is as follows. In the next section we discuss materials synthesis and our experimental setup. We then describe our results, and in the final section discuss the conclusions of our study and future research directions.

II. Materials Synthesis and Experimental Procedures

The MoS_2 nanoclusters were made with an inverse micelle technique. We briefly describe the synthesis here; more detailed descriptions are given elsewhere.[11−13] Inverse micelles are formed when surfactant molecules are dispersed in a nonpolar (e.g., octane, oil) continuous medium. In such a solution, the hydrophilic ends of the surfactant molecules avoid the oil and form droplet-like cages whose sizes typically range from one to tens of nanometers. MoS_2 clusters are formed by first dissolving a molybdenum(IV) halide salt inside the cages and then combining this solution with another inverse micelle solution containing a sulfiding agent (e.g., metal sulfide or H_2S). The synthesis is done in a drybox with catalytic oxygen and water removal to prevent degradation of the Mo(IV) salt precursor. Both oxygen and water levels were monitored and kept below 1 ppm during the reaction. The Mo:S ratio was chosen to be 1:2 or less. The cluster size is varied by using different-sized micelle cages to encapsulate the Mo salt.

Figure 3 shows optical absorption spectra of the MoS_2 nanocluster samples examined in this work. The position of the longest wavelength (direct) absorption feature shifts nanocluster size with MoS_2 (d = 8−10 nm) having this feature at ∼700 nm and MoS_2 (d = 4.5 nm) at ∼470 nm. The absorbance to the red of this peak is due to indirect transitions as discussed in refs 11, 12. The blue shift of absorbance with decreases in nanocluster size changes the color of the clusters from blue (d = 8−10 nm) to red (d = 4.5). Further blue shifts and color

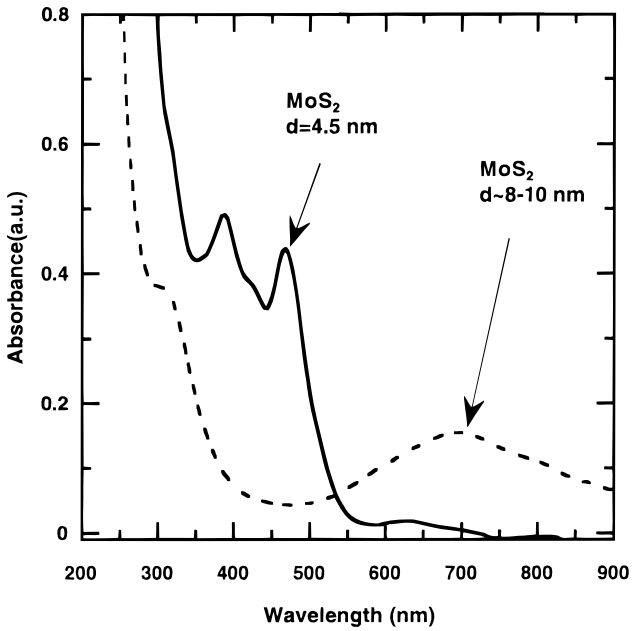

Figure 3. Optical absorption spectra of the MoS_2 ($d = 8-10$ nm) and MoS_2 ($d = 4.5$ nm) nanocluster solutions examined in this work.

changes occur (not shown) as the size decreases to $d = 3.0$ nm yellow-colored solutions. A complete electronic analysis of these features compared to the bulk material is given elsewhere.[12] Previous characterization of these MoS_2 nanoclusters by TEM and dynamic light scattering,[12] was used to establish the nanocluster size and its relationship to the absorbance edge of the clusters. It is interesting to note that the broad absorbance feature at ~700 nm for the $d = 8-10$ nm clusters corresponds to the first direct transition in bulk films of MoS_2,[9] while the absorbance to the red of this is similar to the observed weak indirect transitions that begin at ~1.2 eV (~1000 nm) in the bulk films. So it appears these larger clusters are somewhat bulklike in electronic properties, though they scatter a negligible amount of light because of their small size. As noted previously, the band edge and associated valence and conduction band edges shift to more positive and negative potentials, respectively, and we have estimated the size of these shifts in a previous paper.[14] This potential energy shift provides a larger driving force for oxidation and reduction reactions than in the bulk material.

The stability against agglomeration of MoS_2 nanoclusters in aqueous solution is also size dependent. It turns out that MoS_2 (d ~8−10 nm) nanoclusters are stable in water without surfactant. On the other hand, MoS_2 ($d = 4.5$ nm) though stable without surfactant in a strongly coordinating polar organic solvent like acetonitrile, must be capped with a surfactant of some sort in order to prevent agglomeration in pure water. This situation poses some practical problems, since the surfactant may or may not allow electron/hole transfer. Indeed, the stabilizing surfactant used dodecyltrimethylammonium bromide-poisoned TiO_2 in test experiments. We empirically discovered, however, that the surfactant itself can be photooxidized (into unknown products), and that if the MoS_2 plus surfactant solution were first irradiated for ~12 h with 365 nm radiation, then the presence of the surfactant did not hinder further reactions.

The photooxidation reactor consisted of a 50 mL Pyrex beaker open to air and over which was placed either a 365 nm, 12 W lamp (Spectroline ENF-260C) or a xenon arc lamp operated at 400 W with a long-pass filter in front. The filter allowed 1%, 5%, and 50% transmission at 445, 450, and 455 nm, respectively. The solution was stirred with a magnetic stir bar. The cross-sectional area for light interception was 12.6 cm^2, and the total amount of light intercepted from the 365 nm lamp was 8 mW. The contents were rapidly stirred during the reaction at an identical rate for all samples. Experiments done in a beaker covered with handiwrap using a TiO_2 slurry gave identical reaction kinetics to that of the open beaker, so evaporation on the time scale of the experiments (several hours) was not significant.

Chemical analysis was done with high-pressure liquid chromatography (HPLC) using a Waters Delta Pak, 15 μm particle size, C18−300 Å column, Hewlett-Packard 1050 diode array detector, and Hewlett-Packard 1046A fluorescence detector. The solvent was 50% acetonitrile (Fisher HPLC grade) and 50% H_2O treated with a Millipore milli-Quv plus system, and the flow rate was 1 mL/min. Standard samples of phenol in water at 20 mg/L, 2 mg/L, and 0.2 mg/L in water were prepared and used to obtain the detector(s) response function vs known phenol concentration. The responses were quite linear over this range. The minimum detectable concentration with 50 μL of injected sample was ~0.02 mg/L using the fluorescence detector and exciting the phenol at 250 nm and detecting at the peak emission of ~320 nm. Other aromatic oxidation intermediates were readily identified by their fluorescence response under these excitation conditions. The sample-to-sample phenol elution peak area reproducibility was ±1−2% for independently prepared samples. The area reproducibility for a given light exposure time for the photooxidation experiments for independently prepared catalyst/phenol system was ±5%.

A number of different chemicals including pentacholorophenol and chloroform were photooxidized using nanosize MoS_2, but most of our work focused on the destruction of phenol (Aldrich, >99% pure). This particular substrate was chosen for its ease of detection and good resistance to oxidation, and because its photooxidation has been studied extensively by many previous researchers. No attempts were made to find the absolute quantum yield of the photooxidation process. Rather, following the approach of Serpone et al.,[18] we compared the relative activity of nanosize MoS_2 to a well-studied photocatalyst, Degussa P25 TiO_2. In a typical experiment, 0.08 g of catalyst was added to 40 mL of 20 mg/L phenol solution and stirred for ~30 min in the dark. In the case of both TiO_2 slurries, fully dispersed MoS_2 nanoclusters, and MoS_2 nanoclusters supported on TiO_2 powder, addition of the catalyst resulted in an immediate lowering of the free phenol concentration by ~1−10%, due to adsorption of the phenol on the catalyst. The pH was *not* adjusted by adding acids or bases to the solution, so its value was typically ~7. Before irradiation ($t = 0$), and periodically thereafter, ~1 mL aliquots were removed with a syringe. Large particulates were first removed with 0.22 μm nylon filters, and the samples were then analyzed with HPLC. Separate measurements showed no phenol was removed by the filters used, so the observed phenol elution peak areas were representative of the free phenol concentration in the reactor.

III. Results and Discussion

A. Nanocluster Photostability. As discussed in the Introduction to this paper, defect-free bulk MoS_2 is kinetically resistant to photodegradation.[7,20] However, we noticed that the color of our blue-colored, $d = 8-10$ nm nanosize MoS_2 solutions would oftentimes fade when irradiated with UV light at 365 nm for long periods of time. This color change occurred only when all the stabilizing surfactant was removed from the nanoclusters and only when UV light was used. The smaller, surfactant-stabilized, $d = 4.5$ nm, red-colored, nanocluster solutions showed no optical changes under the same conditions.

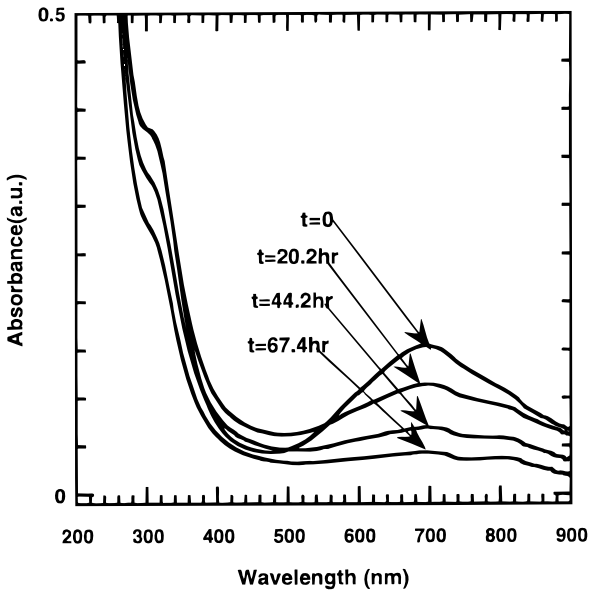

Figure 4. Optical absorption spectra of an aqueous solution of MoS_2 ($d = 8-10$ nm) nanoclusters after being irradiated with 365 nm light for various amounts of time. The absorption between 600 and 900 nm decreases with irradiance time as the solution becomes lighter blue in color.

To explore this issue further, we placed some MoS_2 ($d \sim 8-10$ nm) clusters in aqueous solution (with no protecting surfactant) and then irradiated the solution with 365 nm UV radiation. A control solution that was not irradiated was also prepared. Optical absorption measurements were performed periodically to monitor the condition of the nanoclusters. The results of this study are shown in Figure 4. The intensity of the optical absorption in the visible diminished with time as the sample faded, changing from deep blue to light blue as this process occurred. No precipitates were observed after extended illumination, and there appears to be no shift in the absorption peaks as well. In contrast, the control solution exhibited no changes in color or optical absorption spectra during this same time interval.

The samples shown in Figure 4 were also analyzed for total Mo, S, and dissolved sulfur in the form of sulfides, sulfates, and sulfites. Ion chromatography was used to detect dissolved sulfate ions. Sulfur oxidation to sulfate would occur if the color change observed corresponded to simple chemical oxidation of the nanoclusters, as is known to occur in II−VI nanoclusters such as CdS. We detected identically low levels of dissolved sulfur of 0.001 wt % (an order of magnitude lower than the total sulfur detected) in all four samples of Figure 4, indicating this color change is not due to simple photooxidation of the nanoclusters which would release sulfate ions into the solution.

A possible explanation for the behavior shown in Figure 4 is that the nanoclusters have some unextracted surfactant adsorbed on edge sites which, when exposed to UV light, photooxidize or desorb from the nanoclusters, changing the nanocluster spectra. Some support for the role of adsorbed surfactant molecules on the optical absorbance properties of nanosize MoS_2 comes from our previous studies[14] of strongly bound molecules such as bipyridine. Changes in the relative intensity of the absorbance bands of MoS_2 nanosize semiconductors are observed to occur in this case as bipyridine can easily displace a typical cationic surfactant used for stabilization purposes. We have found that deliberate addition of certain cationic surfactants to nanosize MoS_2 blue-colored solutions results in a change of color from blue to blue-green. Similarly, simple salts such as KI can have the effect of changing the apparent color of the surfactant-free MoS_2 solutions from deep blue to lighter blue-green in color. However, the absorbance features do not change in energy-only the relative extinction of each band change.

Although we cannot completely rule out some type of photochemical degradation in the unprotected, $d = 8-10$ nm MoS_2 nanoclusters upon exposure to UV light, it appears from our chemical analysis that no additional inorganic ions (e.g., sulfate) are being released in this process. One might expect that quantum confinement, which shifts the hole potential of nanosize MoS_2 to more positive potentials, would increase the probability of hole oxidation of the lattice. Mitigating this effect, however, the larger surface area and more defect sites on a nanocluster surface compared to the bulk material increase the number of surface hole traps and apparently prevent photooxidation of the nanoclusters.

B. Phenol Destruction with Visible Light. One of our primary reasons for examining MoS_2 nanoclusters was to try to find a nanoscale photocatalyst that is active when illuminated by visible radiation. In this regard, we were successful, as illustrated in Figures 5, 6, and 7. These chromatographic plots show the attempted photooxidation of phenol with visible radiation by equal concentrations of MoS_2 ($d = 8-10$ nm), MoS_2 ($d = 4.5$ nm), and Degussa P25 TiO_2. The illumination setup, as described above, used a 400 W xenon arc lamp along with a 455 nm long-pass filter. In each case, the catalyst was mixed into ~40 mL of H_2O and illuminated with 365 nm radiation overnight. Four milliliters of 200 mg/L phenol solution and enough H_2O to bring the solution up to 40 mL were then added and after stirring for ~30 min in the dark, illumination with the arc lamp/455 nm filter was initiated. The phenol concentration as a function of time was monitored using HPLC. An important technical note is that the free phenol concentration is plotted in these figures. This is determined at $t = 0$, after addition of the catalyst, but before any illumination. We typically observe a 1−10% decrease in the free phenol concentration just due to adsorption onto the catalyst. This adsorption decrease is largest for the surfactant-free, $d = 8-10$ nm MoS_2 nanoclusters and the least for the TiO_2 powder, where it is basically negligible at the catalyst concentration of 0.1 g/L. However, it is significant for the nanoclusters and was taken into account. Figure 5 shows typical 225 nm absorption chromatograms taken on the MoS_2 ($d = 4.5$ nm) sample run. The peak at ~14.6 min arises from the phenol, and its area decreased by ~25% over a period of ~8 h. There was also a peak at ~15.9 min that was identified (by retention time) as the unbound cationic surfactant used to stabilize these nanoclusters and was absent from both the MoS_2 ($d = 8-10$ nm) and TiO_2 runs. On the other hand, the two peaks at 12.2 and 13.4 min could be identified as phenol oxidation products, since they appear only after the sample was illuminated. One of these peaks, ($t = 13.4$ min) was later identified by retention time to be catechol, presumably resulting from the addition of OH to the aromatic ring. The other peak at $t \sim 12.2$ min is also an aromatic (by its absorbance spectra and fluorescence) and may be an isomer of catechol (i.e., also formed by OH radical addition to phenol). In Figure 6 the chromatogram obtained for $\lambda = 365$ nm illumination of TiO_2 shows the catechol intermediate elution peak, so the reaction mechanism for phenol oxidation by nanosize MoS_2 using visible light may be similar to that previously posited for TiO_2 using UV light.[18] The empty d-orbitals available at Mo metal edge sites on the nanoclusters are quite likely locations for the observed phenol adsorption and hole transfer. Other electron-donating substances such as water or acetonitrile could presum-

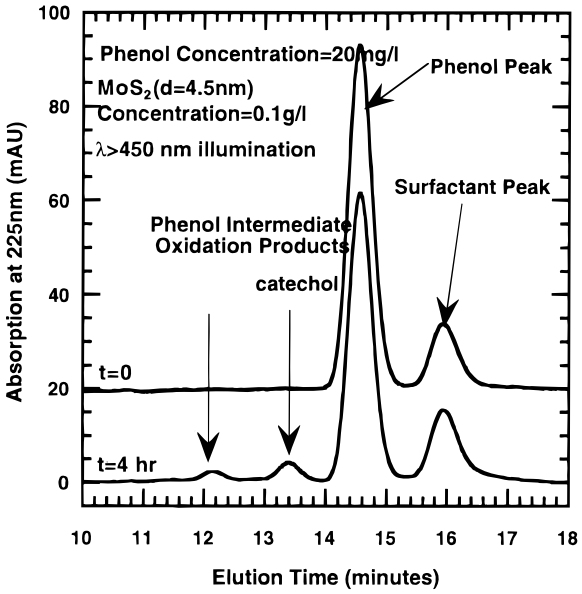

Figure 5. High-pressure liquid chromatrography (HPLC) chromatograms of phenol destruction with visible light catalyzed by MoS_2 (d = 4.5 nm) nanoclusters.

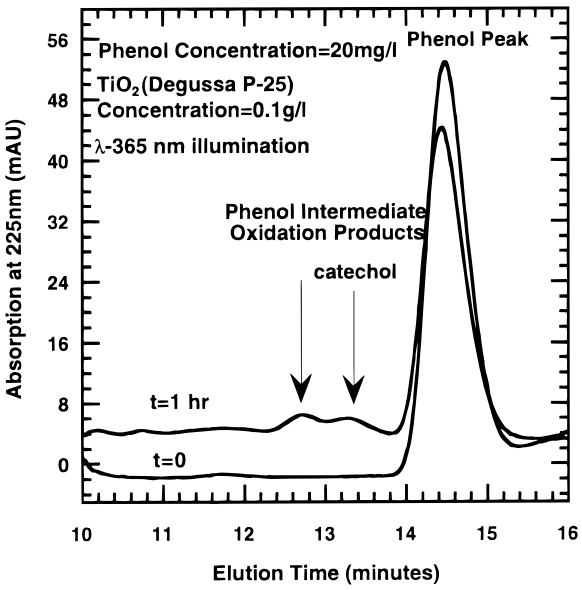

Figure 6. HPLC chromatograms of phenol destruction with λ = 365 nm UV light catalyzed by Degussa P25 TiO_2.

ably also interact with these sites, providing a hole transfer mechanism to water or phenol similar to that observed at Ti(IV) sites in TiO_2.

For these reactions in which the nanosize MoS_2 is fully dispersed it is possible to detect an elution peak at earlier times (not shown) which was identified by its absorbance spectrum to be nanocluster MoS_2. The area of this peak and its complete absorbance spectrum for the surfactant-stabilized, d = 4.5 nm MoS_2 nanoclusters did not decrease during experiments with either visible illumination or 365 nm light, indicating that this sample is acting as a true photocatalyst and it is not being photooxidized.

Figure 7 shows the chromatograms at comparable times under visible illumination where the catalyst was Degussa P25 TiO_2. Not surprisingly, no photooxidation takes place since TiO_2 does not absorb in this region. Unlike Figure 6, where TiO_2 was illuminated with UV light at 365 nm, there are no intermediate product peaks.

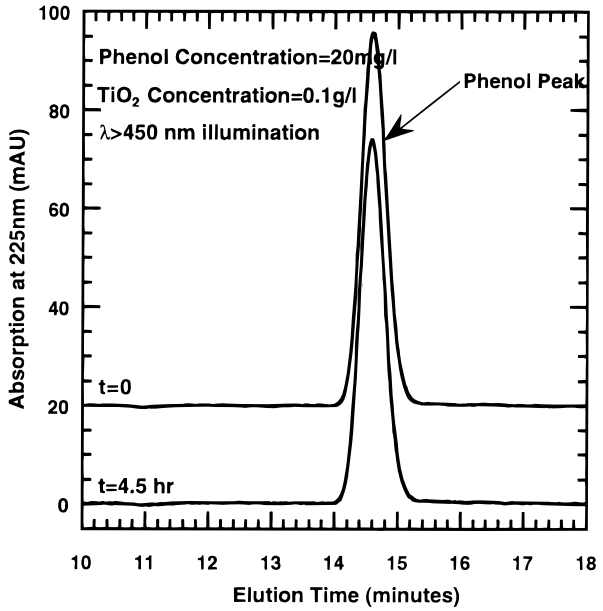

Figure 7. HPLC chromatograms of phenol destruction with visible light catalyzed by Degussa P25 TiO_2.

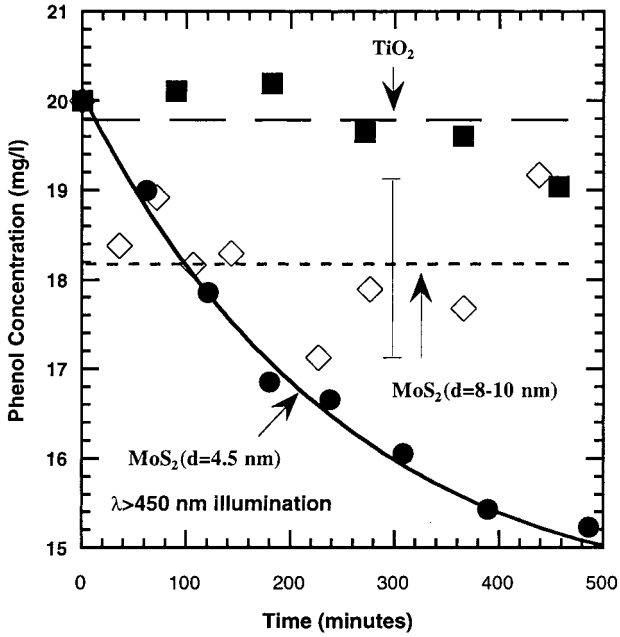

Figure 8. Visible-light-driven phenol oxidation as a function of irradiance time as determined from HPLC chromatograms such as those shown in Figures 5 and 7. The MoS_2 (d = 4.5 nm) nanoclusters catalyze phenol destruction with visible light, while the MoS_2 (d = 8−10 nm) nanoclusters initially adsorb phenol but fail to photooxidize it. Degussa P25 TiO_2 which does not absorb visible light shows no activity as expected. The lines are guides to the eye. The bar is the reproducibility of the HPLC measurements for independent runs.

In Figure 8, we show the phenol concentration as a function of time as determined from chromatograms such as those shown in Figures 5 and 7. Under visible illumination there is a steady decline in the phenol concentration with MoS_2 (d = 4.5 nm) nanoclusters, a reduction in free phenol concentration at t = 0 due to adsorption to the bare MoS_2 (d = 8−10 nm) nanoclusters, and no phenol destruction with Degussa P25 TiO_2. We were able to add additional phenol to the MoS_2 (d = 4.5 nm) nanocluster sample after most of the phenol was destroyed and reproduce the kinetics shown in Figure 8 to within the error bar indicated on this figure.

Two control experiments were also performed. In the first, a 20 mg/L phenol solution was illuminated with the >450 nm setup and no catalyst. In the second, a MoS_2 (d = 4.5 nm) nanocluster solution plus phenol solution identical to that of Figures 7 and 8 was prepared but not illuminated. For each control experiment, no decline in the phenol concentration was observed. Thus, oxidation of the phenol is due to the presence of both MoS_2 catalyst and >450 nm radiation.

Figure 8 is the main result of this work. MoS_2 nanoclusters, if sufficiently small, photocatalyze the destruction of a difficult-to-oxidize compound with visible light. The lack of catalytic activity for the MoS_2 (d = 8−10 nm) solution suggests that its valence band potential has not been shifted to positive-enough values to produce hydroxyl radicals that can oxidize phenol. This observation is similar to experiments we have reported on photoreductive electron transfer from nanosize MoS_2 to bipyridine and tetramethyl substituted bipyridine in which nanocluster size played a critical role in the rate of electron transfer—the smallest clusters giving the fastest rates.[14]

C. MoS_2-Supported Catalysts. Catalytic materials are oftentimes deposited onto support materials. This is done not only to prevent the catalyst from agglomerating, but often because reaction rates can be synergistically increased through interactions between the catalyst and support material. This strategy can be applied to semiconductor photocatalysts and, for MoS_2 nanoclusters, deposition on a support material may increase chemical photostability as well. Also, by combining two different semiconductor photocatalysts we can take advantage of the possibility of electron or hole transfer between the semiconductor catalysts, which could then lead to enhanced electron−hole lifetimes and faster redox reaction rates. This latter possibility was first demonstrated in 1984 by Serpone et al.;[19] another more recent study is given in References.[8]

A series of experiments where MoS_2 (d = 8−10 nm) nanoclusters were deposited onto TiO_2, SnO_2, WO_3, and ZnO were performed. The deposition method was remarkably simple. Powdered support material was mixed into a solution of MoS_2 nanoclusters and then centrifuged with a vacuum applied. The solution slowly evaporated leaving nanoclusters deposited onto the support material. No heating or other treatments were performed, so further future improvements of contact interactions between the nanoclusters and semiconductor support material is possible. With this method it is not clear how uniform a dispersion can be obtained on the powder. In all cases, between 0 and 6 wt % MoS_2 nanoclusters were deposited onto the support. The reaction rate for destruction of 20 mg/L phenol was then measured with a total (MoS_2 + support) catalyst density of 2 g/L.

Figure 9 compares phenol destruction rates for three different loadings of MoS_2 (d = 8−10 nm) on Degussa P25 TiO_2. The 2.5 wt % loaded sample destroyed the phenol faster than the unloaded sample, while the 5 wt % loaded sample was slower. The data in Figure 9 show that the initial destruction rate is a good predictor of the relative phenol concentration at all subsequent times. We therefore shall use the initial destruction rate to summarize relative catalytic activities. To do this, we fit data such as that shown in Figure 9 to the phenomenological form

$$C = \frac{a + bt}{1 + ct}$$

where C is the phenol concentration, t is the time, and a, b, and c are fitting parameters. From such fits, a rough estimate of the initial destruction rate can be found.

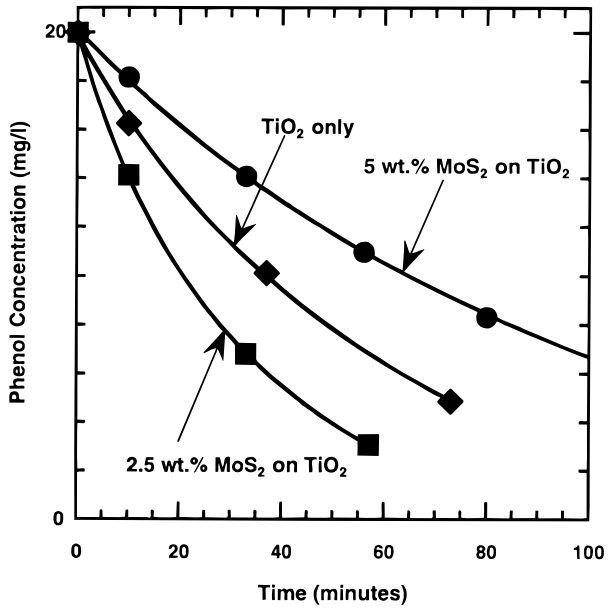

Figure 9. Phenol concentration as a function of time as determined from HPLC chromatograms for Degussa TiO_2 loaded with 0, 2.5 wt %, and 5.1 wt % MoS_2 (d = 8−10 nm) nanoclusters. The radiation wavelength for this set of experiments was 365 nm.

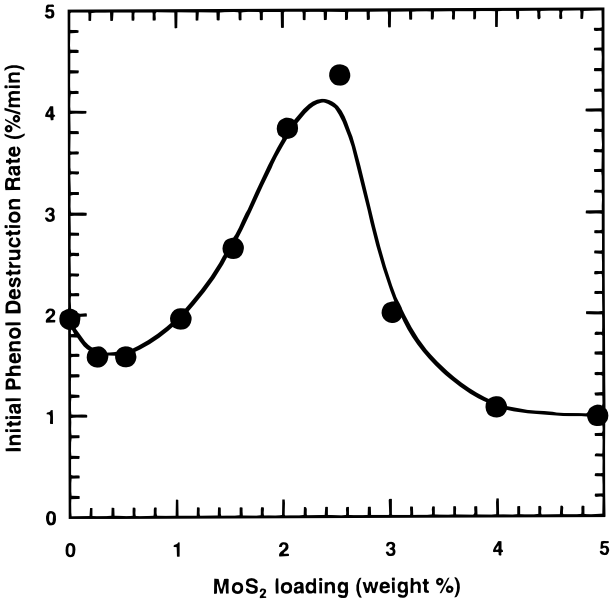

Figure 10. Dependence of the initial phenol destruction rate on the weight percent loading of nanosize MoS_2 (d = 8−10 nm) on Degussa P25 TiO_2. The illuminating radiation was 365 nm and the TiO_2 concentration was 2 g/L in each case.

The initial destruction rate as a function of MoS_2 (d = 8−10 nm) loading is shown in Figure 10. The destruction rate increases with wt % MoS_2 up to a factor of ~2 when the loading is ~2.5 wt %, and it then decreases with further loading. Conversely, in the absence of TiO_2 powder (i.e., dispersed MoS_2 nanoclusters alone at 0.05 g/L) the phenol destruction rate is much smaller. These observations suggest that the nanosize MoS_2 and TiO_2 support are working in a cooperative manner to enhance the electron or hole transfer rate. Similar deposition experiments on other bulk metal oxide powders such as SnO_2, WO_3, or ZnO led to no enhancement in activity over the metal oxide by itself. These powders and other TiO_2 powders are all less active for phenol oxidation under identical reaction conditions than Degussa, P-25 TiO_2.

The decrease in the initial reaction rate for loadings greater than 2.5 wt % is somewhat puzzling. However, similar effects are often observed in traditional thermally activated metal catalysts deposited on metal oxide supports such as alumina, where the optimal metal loading often lies between 1 and 5 wt %. The belief in this case is that excessive metal loading reduces the state of dispersion of the metal (i.e., the available catalytically active surface area), via agglomeration processes during the in situ catalyst synthesis. However, since our supported semiconductor photocatalysts are synthesized in quite a different manner than traditional metal/metal oxide catalyst, a reduced state of dispersion may not be the best explanation in the present case. There may be two competing processes occurring when nanocluster MoS_2 is loaded onto TiO_2, one which enhances phenol destruction and another which impedes it. A possible scenario which would rationalize our observations is that a small amount of deposited MoS_2 enhances phenol destruction through electron or hole transfer processes, but that excess amounts of MoS_2 impede phenol destruction by blocking important phenol binding sites on the TiO_2 surface.

IV. Conclusions

The experimental results presented in this paper demonstrate that nanoscale MoS_2 clusters can photooxidize organic molecules with visible light. The photooxidation of organic molecules occurs in both fully dispersed nanoparticle form and when the nanoclusters are deposited on TiO_2 powder. Effective photooxidation in the dispersed state occurs only for sufficiently small nanoclusters (i.e., $d = 4.5$ nm) whose valence band potential has been shifted to sufficiently positive values by quantum confinement effects. We are currently continuing our photocatalysis studies using $d = 3.0$ MoS_2 nanoclusters whose absorbance begins around 450 nm. Though the more positive valence band potential for these smaller clusters will likely result in a larger rate of hole transfer, they also absorb significantly less visible light.

In any practical application of MoS_2 nanoclusters as photocatalysts, they would have to be supported in a fixed-bed-type flow reactor, and visible light would need to be used as the radiation source to give them an advantage over TiO_2. In dispersed form, though they are convenient for scientific studies, they cannot be effectively removed by filtration or centrifugation from the solvent. However, photocatalysis studies of nanosize MoS_2 in fully dispersed form in combination with HPLC analysis allows one to study both the photocatalyst and reaction products simultaneously, which is a significant advantage over typical TiO_2 slurries.

As a first step to developing a practical form for these new nanocluster photocatalysts we studied supported MoS_2 ($d = 8-10$ nm) nanoclusters and demonstrated enhanced photooxidation of phenol when they were deposited on TiO_2. Similar enhancement effects were absent when these nanoclusters were deposited onto ZnO, SnO_2, and WO_3. As these larger nanoclusters were very inactive by themselves for photooxidation of phenol, these results are quite encouraging. Since MoS_2 ($d = 4.5$ nm) in dispersed form was effective for phenol oxidation using visible light, we are currently examining the effect of deposition of these nanoclusters onto TiO_2 for the photocatalytic oxidation of pentachlorophenol.

In the future we want to explore other surface modifications of our nanoclusters including heat treatments of the MoS_2/TiO_2 powders to improve the chemical interaction between the two semiconductors and would like to deposit metals such as Co or Ni onto the nanosize MoS_2.

Acknowledgment. This work was supported by the Environmental Management Science Program of the U.S. Department of Energy under contract DE-AC04-AL8500. Sandia is a multiprogram laboratory operated by Sandia Corporation, a Lockheed−Martin Company, for the U.S. Department of Energy.

References and Notes

(1) Fox, M. A.; Dulay, M. T. *Chem. Rev.* **1993**, *93*, 341.
(2) Legrini, O.; Oliveros, E.; Braun, A. M. *Chem. Rev.* **1993**, *93*, 671.
(3) Serpone, N. *Res. Chem. Intermed.* **1994**, *20*, 953.
(4) Hagfeldt, A.; Grätzel, M. *Chem. Rev.* **1995**, *95*, 49.
(5) Hoffmann, M. T.; Martin, S. T.; Choi, W.; Bahnemann, D. *Chem. Rev.* **1995**, *95*, 69.
(6) Linsebigler, A. L.; Lu, G.; Yates, J. T., Jr. *Chem. Rev.* **1995**, *95*, 735.
(7) Tributsch, H. *Z. Naturforsch.* **1977**, *32a*, 972.
(8) Serpone, N.; Maruthamuthu, P.; Pichat, P.; Pelizzetti, E.; Hidaka, H. *J. Photochem. Photobiol. A: Chem.* **1995**, *85*, 247.
(9) Pelizzetti, E.; Borgarello, E.; Serpone, N.; Gratzel, M. *Stud. Surf. Sci. Catal.* **1984**, *19*, 327.
(10) Tributsch, H.; Pohlmann, L. *Science* **1998**, *279*, 1891.
(11) Wilcoxon, J. P.; Samara, G. A. *Phys. Rev. B* **1995**, *51*, 7299.
(12) Wilcoxon, J. P.; Newcomer, P.; Samara, G. A. *J. Appl. Phys.* **1997**, *81*, 7934.
(13) Wilcoxon, J. P. U.S. Patent 5,147,841, September 15, 1992.
(14) Parsapour, F.; Kelley, D. F.; Craft, S.; Wilcoxon, J. P. *J. Chem. Phys.* **1996**, *104*, 1.
(15) Serpone, N.; Khairutdinov, R. F. *Semiconductor Nanoclusters-Physical, Chemical, and Catalytic Aspects*; Kamat, P. V., Meisel, D., Eds.; Elsevier: Amsterdam, 1997; p 417.
(16) Pelizzetti, E.; Visca, M. *Energy Resources through Photochemistry and Catalysis*, Gratzel, M., Ed.; Academic Press: NewYork, 1983; p 261.
(17) Wilcoxon, J. P.; Williamson, R. L.; Baughman, R. *J. Chem. Phys.* **1993**, *98*, 9933.
(18) Serpone, N.; Sauve, G.; Koch, R.; Tahiri, H.; Pichat, P.; Piccinini, P.; Pelizzetti, E.; Hidaka, H. *J. Photochem. Photobiol. A: Chem.* **1996**, *94*, 191.
(19) Serpone, N.; Borgarello, E.; Gratzel, M. *J. Chem. Soc., Chem. Commun.* **1984**, 342.
(20) Pandey, R. K. *Handbook of Semiconductor Electrodepostion*; Marcel Dekker Inc.: New York, 1996; Chapter 7.